J. Membrane Biol. 93, 43–53 (1986)

The Journal of
Membrane Biology

Kinetics of Ultrastructural Changes during Electrically Induced Fusion of Human Erythrocytes

D.A. Stenger and S.W. Hui
Electron Optics Laboratory, Biophysics Department, Roswell Park Memorial Institute, Buffalo, New York 14263

Summary. The sequence of events during the electrically induced fusion of human erythrocytes was studied by rapid quench freeze-fracture electron microscopy. A single electric field pulse was used to induce fusion of human erythrocytes treated with pronase and closely positioned by dielectrophoresis. The electronic circuit was coupled to a rapid freezing mechanism so that ultrastructural changes of the membrane could be preserved at given time points. Pronase treatment enabled adjacent cells to approach each other within 15 nm during dielectrophoresis. The pulse caused a brief disruption of the aqueous boundaries which separated the cells. Within 100 msec following pulse application, the fracture faces exhibited discontinuous areas which were predominantly free of intramembranous particles. At 2 sec after the pulse, transient point defects attributed to intercellular contact appeared in the same membrane areas and replaced the discontinuous areas as the predominant membrane perturbation. At 10 sec after the pulse, the majority of the discontinuous areas and point defects disappeared as the intercellular distance returned to approximately 15 to 25 nm, except at sites of cytoplasmic bridge formation. Intramembranous particle clearing was observed at 60 sec following pulse application in discrete zones of membrane fusion.

Key Words electropermeation · electrofusion · freeze-fracture · intramembranous particles

Introduction

Electrically induced cell fusion and electropermeation have recently become powerful techniques in cell and molecular biology. At this time, the mechanisms of these processes are not well understood. Zimmermann (1982) has provided the most comprehensive model describing the mechanism of electrofusion. According to this model, a large number of pores are simultaneously produced in the lipid domains of closely positioned cells. These pores allow for lipid exchange and subsequent fusion. This process is dependent upon the formation of protein-free regions of the membrane. One result of such perturbation of the membrane would be vesicle formation from isolated membrane fragments. This model is based upon a variety of experimental results. First, the reversible dielectric properties of lipid bilayers upon the application of field pulses may be attributed to large populations (10^6 to 10^7/mm^2) of transient aqueous pores (Benz et al., 1979; Weaver et al., 1984). Many authors have proposed mechanisms for generating such pores in the lipid matrices of cell membranes (for review *see* Dimitrov & Jain, 1984). Second, electrofusion of large unilamellar vesicles composed of pure lipids occurs within several seconds (Buschl et al., 1982), supporting the prediction that fusion is initiated in lipid domains. Third, there are at least two reported instances where electrofusion has been accompanied by vesicle formation (Sowers, 1983; Vienken et al., 1983).

Conductivity characteristics of erythrocyte suspensions suggest a two-stage process of electropermeation (Kinosita & Tsong, 1979), with a significant fraction of the enhanced ion permeability being attributed to the electrogenic nature of the Na,K-ATPase (Teissie & Tsong, 1980). A small number (1 to 10 per cell) of metastable pores (diameter less than 2 nm) are estimated to exist for hours following field pulse application at 0 to 2°C (Schwister & Deuticke, 1985).

The implications of these phenomena in the electrofusion of human erythrocytes remains unclear. Sowers (1985) has suggested that there may not necessarily be a simple relationship between the mechanism of electrofusion and electrically induced pore formation, because human erythrocyte ghosts remain susceptible to fusion by dielectrophoresis alone for as long as several minutes following pulse application in the absence of an alternating current (AC) field (Sowers, 1984).

This study is undertaken to provide an experimental observation of the ultrastructural kinetics of an electrofusion process in a well-characterized

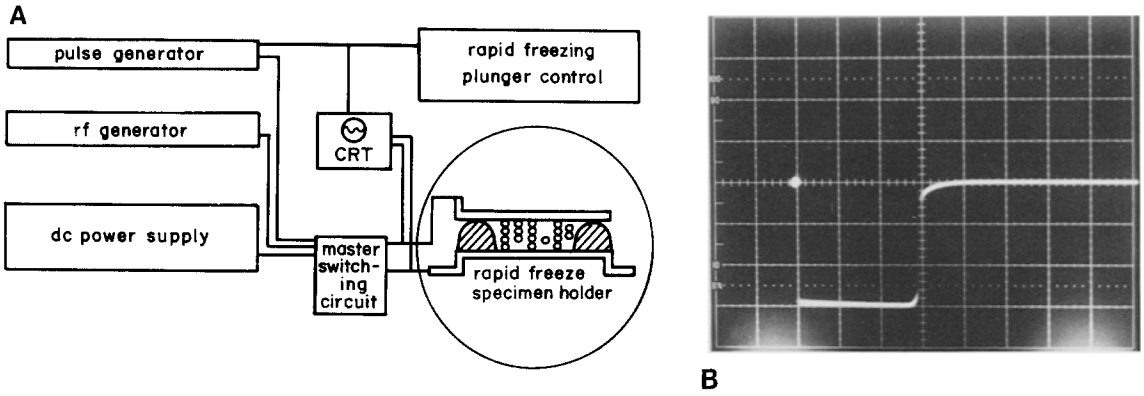

Fig. 1. (*A*) Schematic of electronic setup. (*B*) Electric field pulse across the rapid freeze specimen holder. The specimen holder is shown in an enlarged scale within the circle in (*A*). The shaded mounds and small circles represent the insulation strips and pearl-chained erythrocytes, respectively. The oscilloscope trace is calibrated at 1 V and 1 μsec per small division. The 15 V, 15 μsec pulse shown in (*B*) generated a 5-kV/cm field across the specimen

system. Our experimental data would help to define the sequence of events depicted by various models.

Materials and Methods

Cell Preparation

Human erythrocytes were separated from freshly drawn whole blood, washed twice in balanced salt solution (BSS) at pH 7.4, and incubated at 37°C for 30 min in BSS containing 3 mg/ml pronase E (Sigma Chemical Co., St. Louis, Mo.). The pronase was listed as 15% calcium acetate by weight. The cells were then washed twice again with BSS and then twice with 0.3 M sucrose prior to final resuspension in 0.3 M sucrose at a packed cell : 0.3 M sucrose ratio of 1 : 64 vol/vol and 1 : 2 vol/vol for phase and electron microscopy, respectively. The specific conductivities of representative final suspensions were found to increase from 4.7 $\times 10^{-5}\ \Omega^{-1}\ cm^{-1}$ to 7.3 $\times 10^{-5}\ \Omega^{-1}\ cm^{-1}$ within 60 min. The pH rose from 5.5 to 6.8 during the same period. Therefore, individual suspensions were held on ice and used within 40 min.

Degradation of membrane proteins by the pronase treatment was analyzed by sodium dodecyl sulfate (SDS) gel electrophoresis using the method of Fairbanks et al. (1971). Ghosts were prepared from intact erythrocytes which were subjected to the preparation described above, but not resuspended in 0.3 M sucrose.

Electronic Equipment

The electronic setup used in all experiments is illustrated in Fig. 1*A*. A master switching circuit was used to control the AC and pulsed electric fields across copper specimen holders for rapid freezing. The two sides of the copper sandwich were used also as electrodes. A separation of 25 to 30 μm was created between the electrodes with thin strips of insulation. A pulse generator (model 3300, Dynascan Corp., Chicago, Ill.) was used to control a mercury switch in the switching circuit. Normally, the switch was in the open position, which allowed for the continuous application of a high frequency AC field supplied by a radio frequency generator (model 3025, Dynascan Corp.). When the pulse generator was triggered, it disconnected the AC circuit for a total of 1.5 msec, allowing high field pulse application. The mercury switch then connected the direct current power supply (type 1205-b, General Radio Co., Cambridge, Mass.) at a set delay time, for a period controlled by the selected pulse width. The high field pulse shape was monitored by an oscilloscope (Model 465, Tektronix Corp., Beaverton, Ore.). A 5-kV/cm, 15-μsec pulse across a specimen holder is illustrated in Fig. 1*B*.

Determination of Fusion Protocol

The optimal conditions for fusion by a single pulse were determined by phase microscope observation. The cells were introduced to a light microscope fusion chamber consisting of two platinum or copper electrode strips spaced at a distance of 30 μm. Pearl chains were formed by dielectrophoresis using a 0.5 kV/cm rms AC field for 30 sec. Fusion was then initiated by applying between one and four pulses of 4- or 15-μsec duration. When multiple pulses were used, they were delivered at a rate of 2/sec. The criterion set for a positive fusion event was that two or more cells exhibit no visible cytoplasmic separation within 60 sec of pulse application and that such an attachment remained after the AC field was turned off. A positive trial was defined by at least 50% of the cells aligned in pearl chains exhibiting events satisfying the fusion criterion.

Freeze-Fracture Electron Microscopy

For rapid freezing, 1.0 μl of cell suspension was placed on the bottom surface of the holder and then sandwiched between the prepositioned top surface of the holder by surface tension. Specimen holders loaded as such exhibited a resistance between 100 and 500 kΩ and an apparent capacitance of 1 to 2 mF. The absence of ice damage in the samples indicated that the separation was generally less than 30 μm. The AC field was applied at the set strength for 30 sec prior to pulse application. For observation of the cells within 100 msec following the pulse, the rapid-freeze plunger and pulse generator were simultaneously activated. The drop time of the plunger was calibrated by strobe light photography. A delayed trigger time for the pulse was used to control the duration between the pulse and the time of sample-coolant contact. For longer times following pulse application, the samples were left in position for a set time prior to plunger activation. The rapid-freezing procedure and subsequent freeze-fracture, using the sandwich method, were previously described

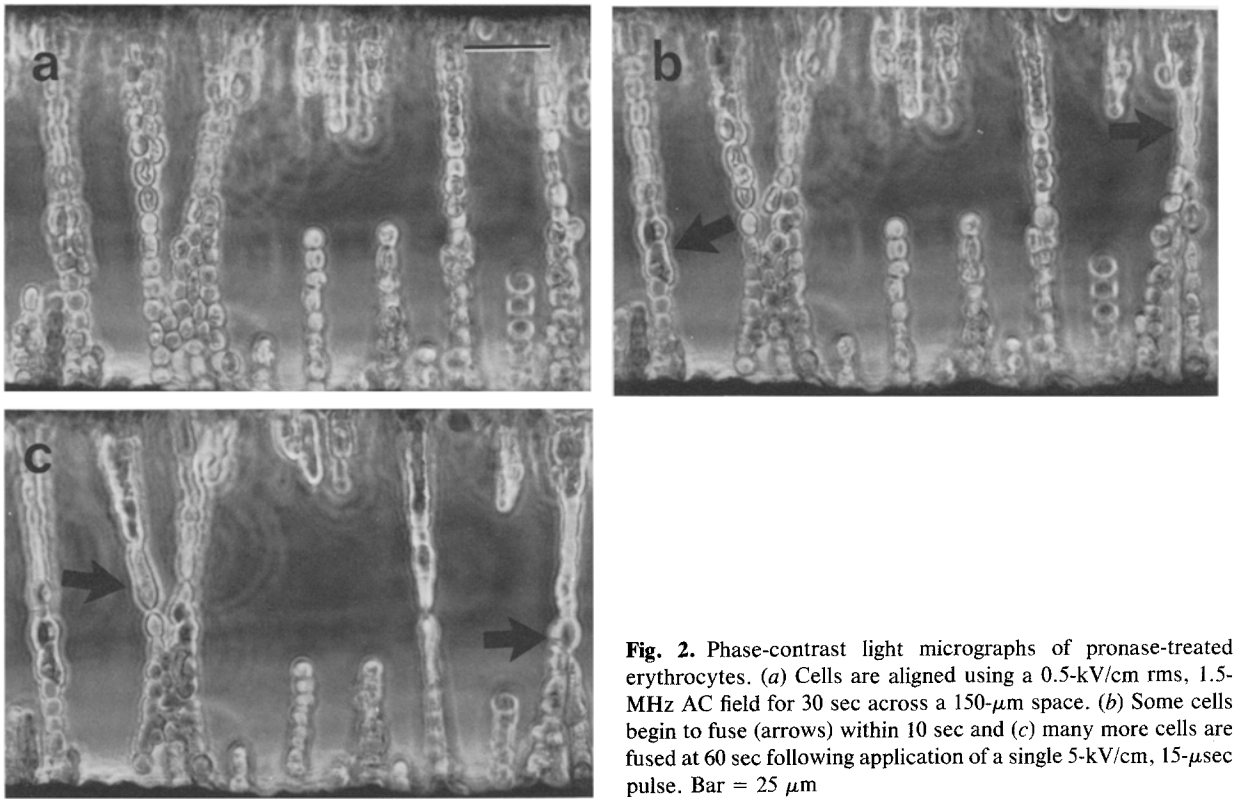

Fig. 2. Phase-contrast light micrographs of pronase-treated erythrocytes. (*a*) Cells are aligned using a 0.5-kV/cm rms, 1.5-MHz AC field for 30 sec across a 150-μm space. (*b*) Some cells begin to fuse (arrows) within 10 sec and (*c*) many more cells are fused at 60 sec following application of a single 5-kV/cm, 15-μsec pulse. Bar = 25 μm

(Costello & Corless, 1978; Hui et al., 1981). Cells which were not treated with pronase, and cells which were treated with pronase but subjected to the high voltage pulse in the absence of an AC field, were used in control experiments. All experiments were performed at room temperature.

Results

Unless otherwise specified, all cells were treated with pronase. The only major proteolytic effect of the treatment on membrane proteins was the degradation of band III (95 kilodalton) protein into two fragments as revealed by our SDS gel electrophoresis analysis results (*not shown*), in agreement with those obtained in previous studies (Cabantchik & Rothstein, 1974).

Several combinations of pulse duration, voltage, and repeat times were experimented to optimize the fusion condition. A positive fusion observed by phase-contrast microscopy is shown in Fig. 2. Prior to pulse application, many cells which were aligned in pearl chains (Fig. 2*a*), began to fuse at 10 sec following the pulse (Fig. 2*b*), and continued to fuse at 60 sec following pulse application (Fig. 2*c*). It was found that, when using a 4-μsec pulsewidth, a minimum of 2 pulses were required for a positive fusion, even when the field strength

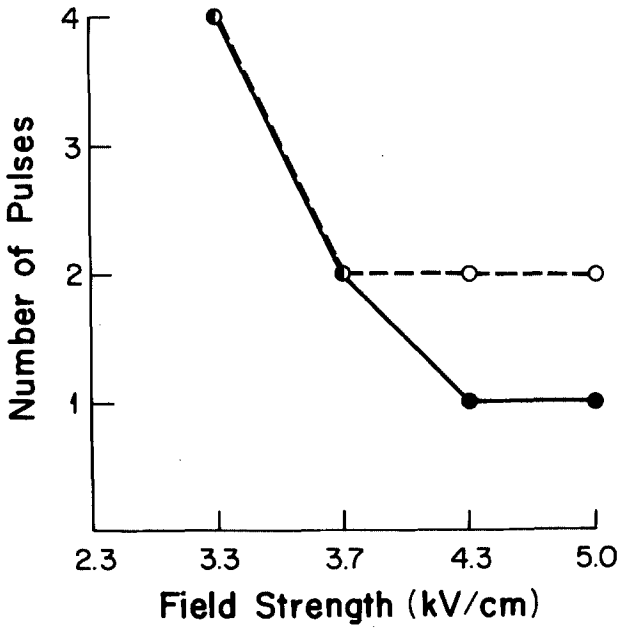

Fig. 3. A plot of the threshold number of pulses necessary for fusion of pronase-treated erythrocytes as a function of pulse-width and amplitude using 4-μsec (○----○) or 15-μsec (●——●) pulses

was increased to 5 kV/cm (Fig. 3, dashed line). However, a single 15-μsec pulse led to positive fusion at both 4.3 and 5 kV/cm (Fig. 3, solid line).

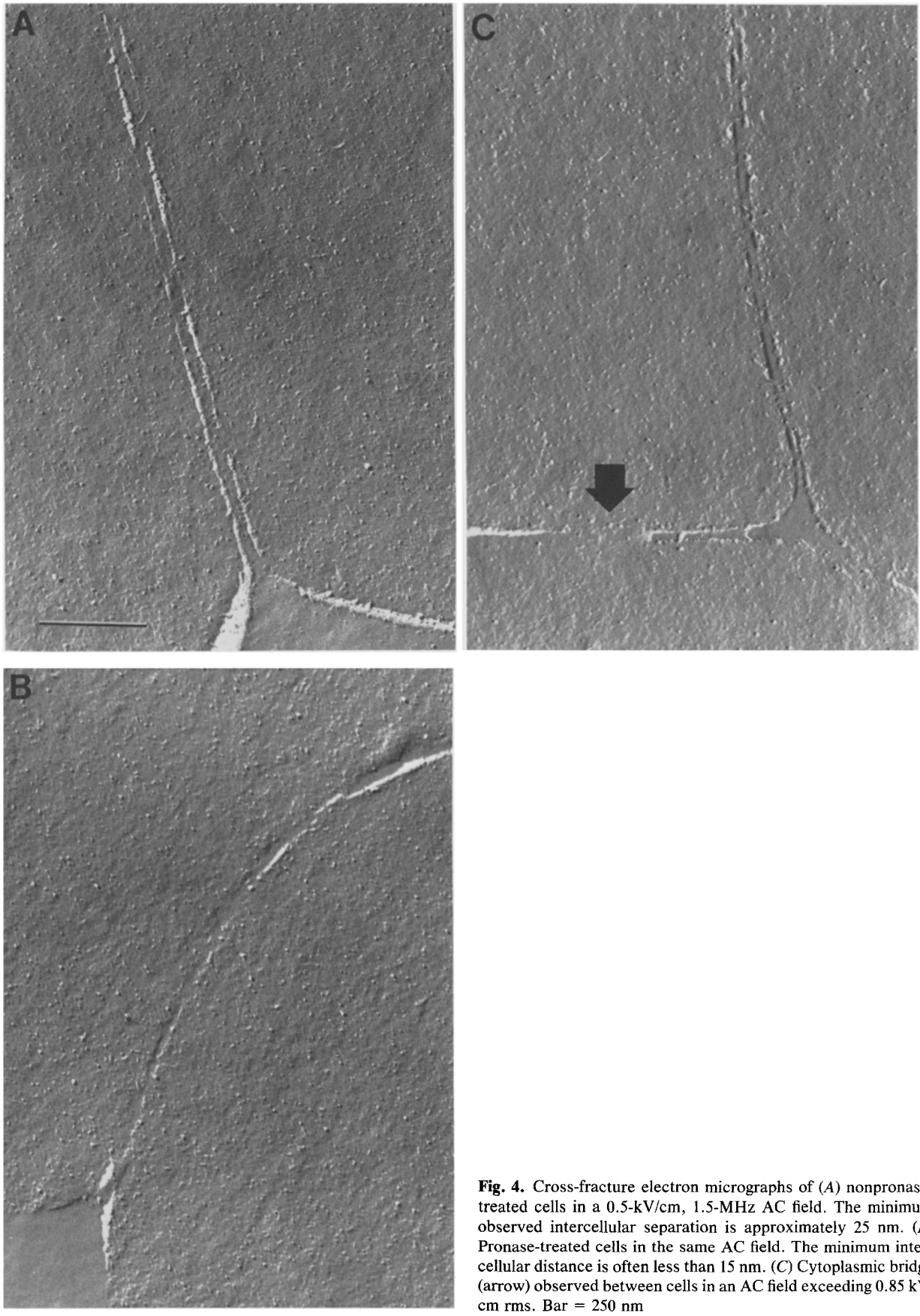

Fig. 4. Cross-fracture electron micrographs of (*A*) nonpronase-treated cells in a 0.5-kV/cm, 1.5-MHz AC field. The minimum observed intercellular separation is approximately 25 nm. (*B*) Pronase-treated cells in the same AC field. The minimum intercellular distance is often less than 15 nm. (*C*) Cytoplasmic bridge (arrow) observed between cells in an AC field exceeding 0.85 kV/cm rms. Bar = 250 nm

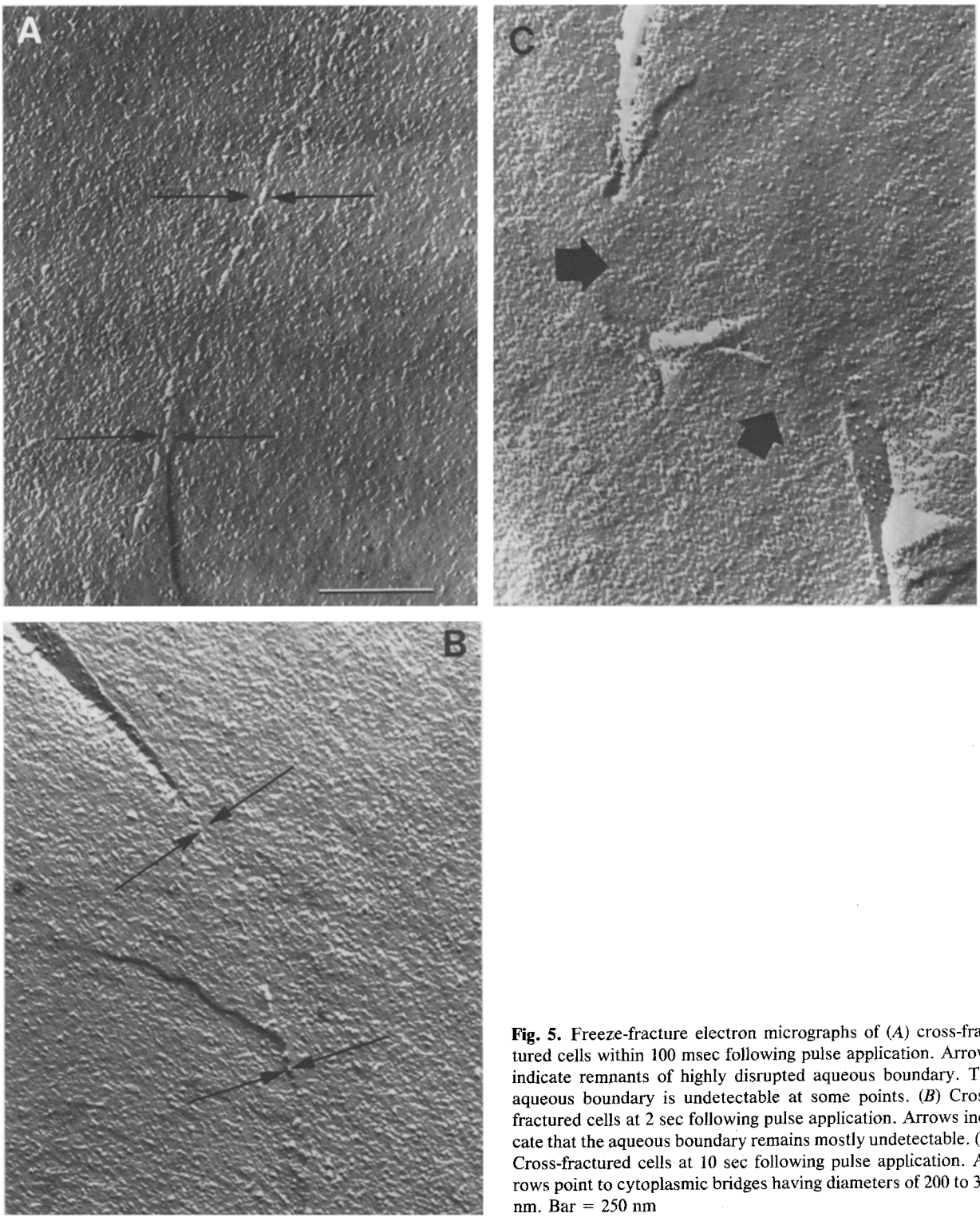

Fig. 5. Freeze-fracture electron micrographs of (*A*) cross-fractured cells within 100 msec following pulse application. Arrows indicate remnants of highly disrupted aqueous boundary. The aqueous boundary is undetectable at some points. (*B*) Cross-fractured cells at 2 sec following pulse application. Arrows indicate that the aqueous boundary remains mostly undetectable. (*C*) Cross-fractured cells at 10 sec following pulse application. Arrows point to cytoplasmic bridges having diameters of 200 to 300 nm. Bar = 250 nm

Therefore, a single 5-kV/cm, 15-μsec pulse was used for all rapid-freeze experiments.

When cells were rapidly frozen during dielectrophoresis, cross fractures revealed that they were always separated by a well-defined aqueous boundary. The minimum observed intercellular distance when using a 0.5-kV/cm rms AC field was approximately 25 nm when the cells were not treated with pronase (Fig. 4*A*). Following pronase treatment, the minimum observed intercellular distance was re-

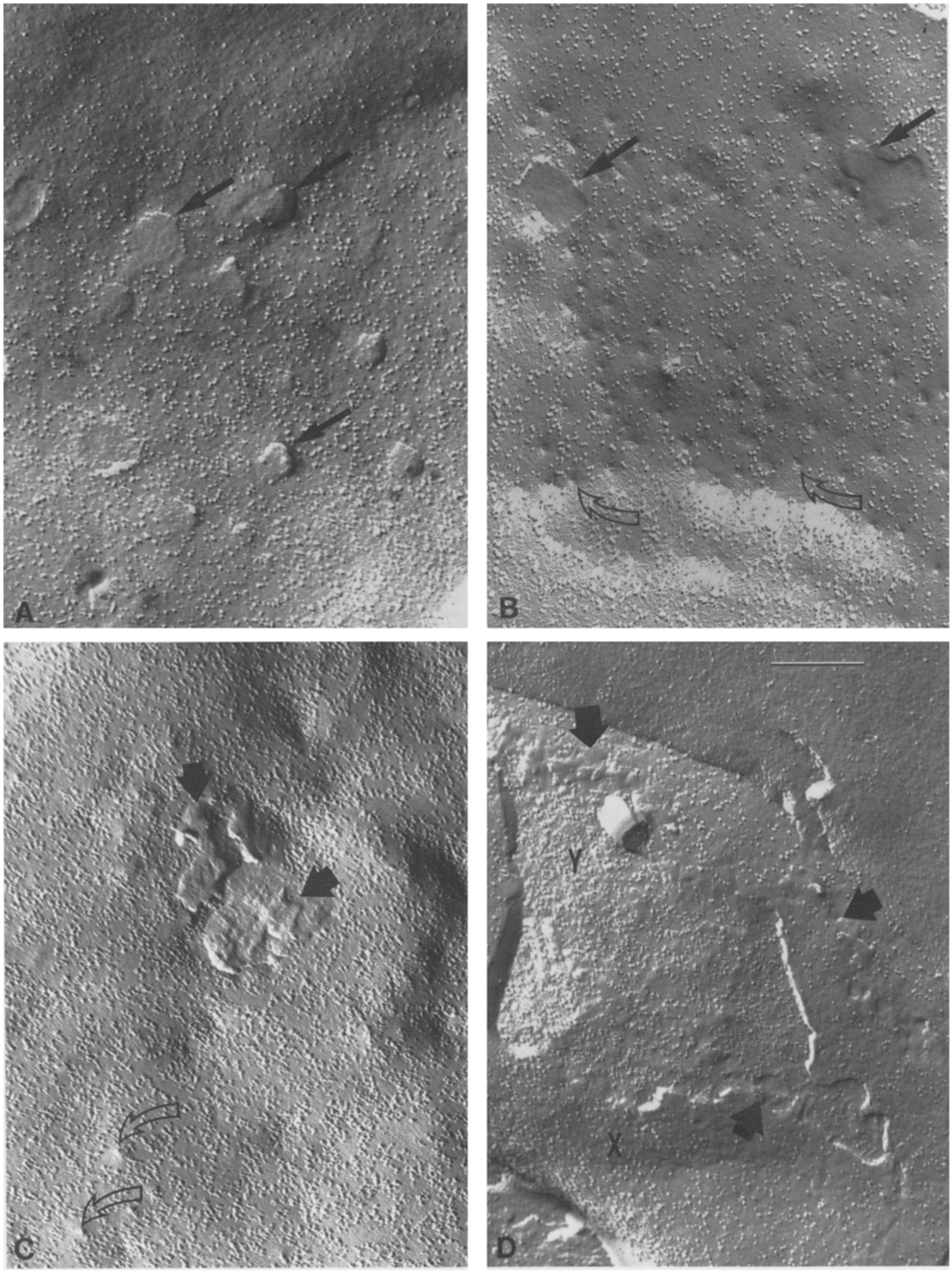
A
B
C
D
Y
X

duced to <15 nm at the same AC field strength (Fig. 4*B*). As long as the AC field strength was kept at or below 0.5 kV/cm, no fusion was observed as a result of the AC field alone. Fusion was occasionally observed between pronase-treated cells when subjected to AC field strengths in the range of 0.7 to 0.85 kV/cm rms, but except at the points of cytoplasmic bridge formation (Fig. 4*C*), the minimum observed intercellular distance remained at approximately 15 nm.

When applying a 0.5-kV/cm AC field prior to and following high voltage application, fusion was readily obtained following application of a single, 15-μsec, 5-kV/cm pulse. Within 100 msec following pulse application, many aqueous boundaries were disrupted and the intercellular separation often became undetectable by freeze fracture (Fig. 5*A*). Face fractures (Fig. 6*A*) showed that discontinuous areas (diam. 50 to 150 nm) projected from the fracture faces. These were the predominant membrane disturbances observed at this time point. Most of the projected discontinuous areas were noticeably free of intramembranous particles (IMPs), and also appeared to be somewhat delimited by the boundaries of the IMP-free areas. Furthermore, the discontinuous areas were asymmetrical in the sense that they always appeared continuous with the plane of the membrane along one edge.

At 2 sec following pulse application, cross fractures showed that the aqueous boundary separating adjacent cells was still undetectable across extended surface areas. Many adjacent cells still had no detectable separation (Fig. 5*B*). However, the face fractures at this time point (Fig. 6*B*) showed that many discontinuous areas were replaced by point defects (diam. 20 to 50 nm) as the predominant membrane perturbation. These point defects bore a strong resemblance to the lipidic particles in phospholipid model systems (Hui et al., 1981; Verkleij, 1984). The occurrence of these defects was for the most part confined to flat or depressed regions of the membrane where two cells presumably were either very closely positioned or in direct contact. The emergence and disappearance of the point defects in the time range of 2 to 10 sec following pulse application suggested that they were indicative of a later occurring event. It is noteworthy that few if any of the discontinuous areas or point defects were observed if the pronase-treated cells were stored at 4°C in BSS for one hour or more prior to the experiment. Under these conditions, fusion efficiency was greatly reduced.

At 10 sec following pulse application, cross fractures showed two prominent features. First, well-defined cytoplasmic bridges were formed having lumen diameters of 300 to 450 nm (Fig. 5*C*). Second, the minimum observed intercellular distance returned to that observed during dielectrophoresis but prior to pulse application, except in points of direct contact at the cytoplasmic bridges. Face fractures at 10 sec following the pulse showed a corresponding loss of point defects (Fig. 6*C*) and development of turbulent membrane disruptions, presumed to be the sites of the initial membrane fusion which were developing into cytoplasmic bridging points.

At 60 sec following pulse application, some cytoplasmic bridges having the same dimensions and morphology as those observed at 10 sec were still present (*not shown*). However, broad areas of membrane fusion were also frequently observed. When viewed along the pearl chain axis, membrane fusion could be seen continuously from the E-face of one cell to the P-face of an adjacent cell (Fig. 6*D* arrows) as IMPs are excluded from the fusion areas. The vanishing of the intercellular aqueous gap into membrane continuity between adjacent cells is illustrated as a montage (Fig. 7).

In order to quantitatively establish the sequence of occurrence of these morphological features, the number of cells exhibiting the above characteristic features at each time point were counted from several representative replicas from four repeating experiments. Figure 8*A* shows the percentages of pronase-treated cells which manifested the face fracture characteristics at various time points. Within 100 msec after the pulse, the predominant features were the discontinuous areas, with 21% of all fracture faces showing this feature. By 2 sec, a decrease in the appearance of discontinuous areas was accompanied by an increase in point defects. Both of these features subsided at 10 sec when the

Fig. 6. (*facing page*) Freeze-fracture electron micrographs of (*A*) E-face fracture at 100 msec following pulse application. Arrows point to discontinuous areas which are predominantly free of IMPs. (*B*) E-face fracture at 2 sec following pulse application. Dark arrows point to several surviving discontinuous areas. Light arrows indicate transient point defects. (*C*) P-face fracture at 10 sec following pulse application. Large arrows indicate an expanding cytoplasmic bridge. Light arrows indicate surviving point defects. (*D*) Face fracture of the contact area between two cells when viewed along the pearl-chain axis at 60 sec following pulse application. The E-face of the top cell, X, becomes continuous with the P-face of the bottom cell, Y, at positions indicated by the arrows. The low proportion of IMPs in these fusion zones suggests that their exclusion precedes lipid exchange between membranes. Bar = 250 nm

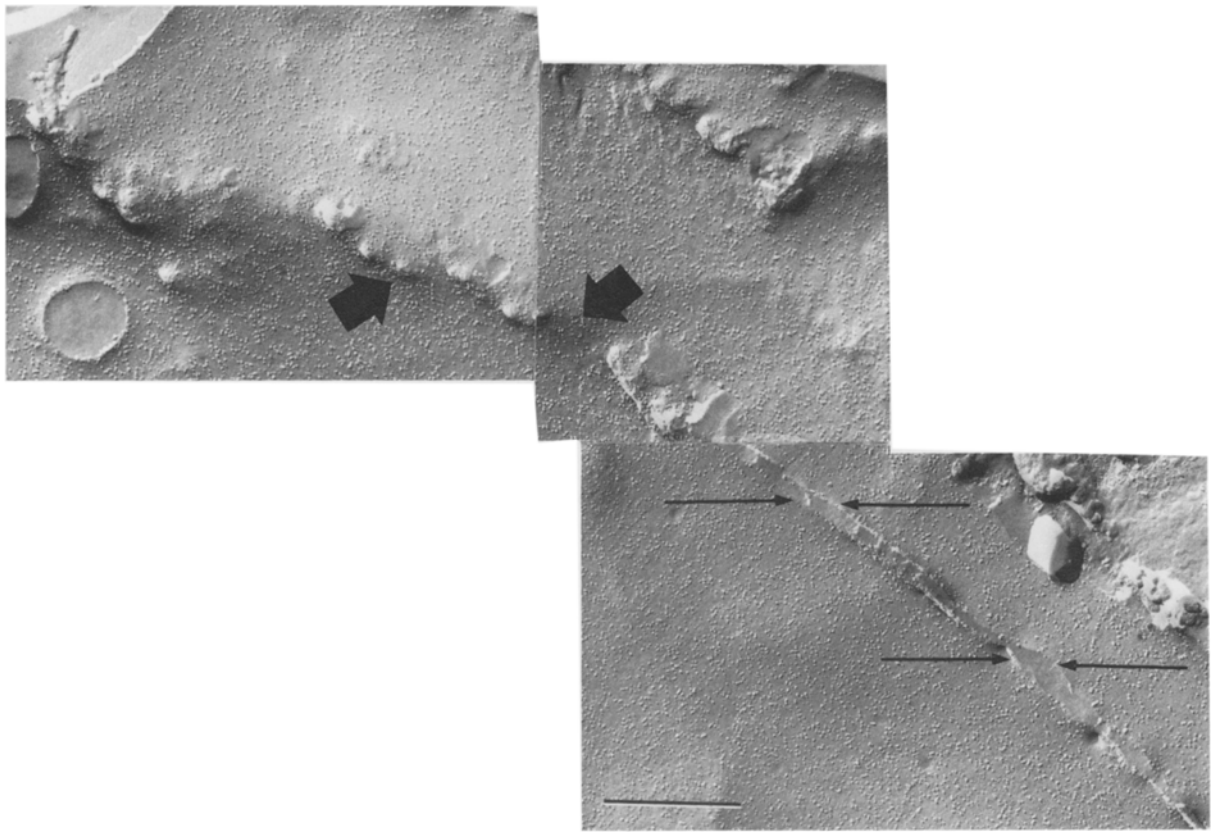

Fig. 7. Freeze-fracture electron micrograph illustrating fusion between two E-face fractured erythrocytes at 60 sec following pulse application. Thin arrows indicate extracellular sucrose solution. Wide arrows in the upper left corner denote regions where membrane continuity has developed. Bar = 500 nm

frequency of membrane fusion increased. Cross-fracture features were quantitated in a similar manner, but only those cells which were within 25 nm of another cross-fractured cell were included in this category. Figure 8*B* shows the percentages of concomitant cross-fracture features under the same conditions. Very close membrane positioning (undetectable aqueous border) occurred with the highest frequency at 100 msec and 2 sec following the pulse. At 10 sec, the percentage of cytoplasmic bridges increased, but otherwise, the frequency of very close positioning greatly decreased.

When cells which were not treated with pronase were subjected to the same fusion protocols as described above, several important differences were observed (Table). While the percentage of cells having discontinuous areas appeared to increase from that under the optimal fusion condition, both at 100 msec and 2 sec following the pulse, the percentage of cells in very close position was very much decreased. At 2 sec following pulse application, there were much less frequent appearances of very closely positioned cells and cells having point defects, as compared to cells under the optimal fusion condition. When pronase-treated cells were subjected to the same electric pulse in the absence of an AC field, the percentage of cells exhibiting discontinuous areas at 100 msec and 2 sec was again much higher than that of cells under the optimal fusion condition. Fewer cells exhibited point defects and very close positioning. Neither cytoplasmic bridging nor membrane fusion were observed in the control experiments.

Discussion

Many studies of membrane electrofusion have been reported, yet there is no ultrastructural evidence of the sequential events happening during the process. Our rapid-freezing study shows that the process may continue for more than one minute, although the initial destabilization requires less than 100 msec. The subsequent steps are not exactly synchronized, as shown by the data in Fig. 8. Thus, the sequence of events can only be reconstructed by

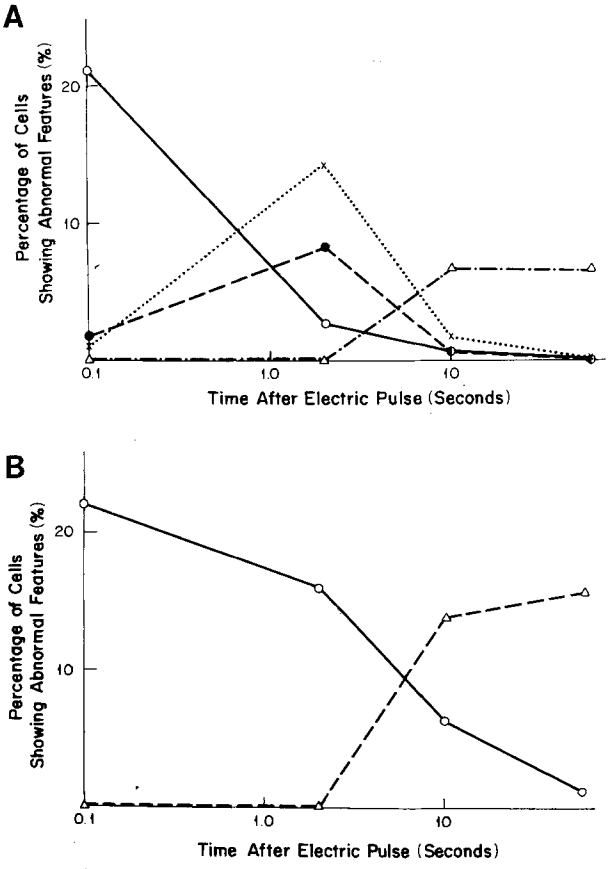

Fig. 8. (*A*) The percentage of pronase-treated cells showing abnormal face fracture features as a function of time following pulse application under optimal fusion conditions; discontinuous areas only (●—●), discontinuous areas + point defects (●--●), point defects only (X·····X), membrane fusion (△-·-△). (*B*) The percentage of pronase-treated cells showing abnormal cross-fracture features as a function of time following pulse application under optimal fusion conditions; very close positioning (undetectable aqueous boundary) (○—○), cytoplasmic bridging (△--△)

Table. Percentages of morphological feature types at given lapsed times after the applied electric pulse

Time	*n*	Face-fracture features			Cross-fracture features	
		% da[a]	% da + pd[b]	% pd	*n*	% vcp[c]
Optimal fusion condition						
0.1 sec	387	21.1	1.8	1.0	129	22.0
2 sec	335	2.7	8.3	14.0	112	16.0
Omitting pulse						
	355	0.05	0.0	0.0	119	0.0
Omitting pronase treatment						
0.1 sec	333	33.5	0.43	0.21	111	2.7
2 sec	342	10.6	0.0	0.73	114	0.0
Omitting AC field						
0.1 sec	348	49.0	1.1	0.5	116	1.7
2 sec	306	11.2	2.5	3.0	102	1.8

[a] da: discontinuous areas.
[b] pd: point defects.
[c] vcp: very close positioning.

sampling at various time points, with statistical uncertainty. Our sample size is sufficiently large to conclude the sequential events.

Cell fusion requires close juxtapositioning and destabilization of cells. Electrofusion protocols satisfy the first of these requirements by dielectrophoresis or high suspension densities (Zimmermann, 1982), contact in culture dishes (Blangero & Teissie, 1983), or by receptor-mediated aggregation (Lo et al., 1984). Repulsive forces (Rand, 1981) apparently oppose direct lipid bilayer contact between dielectrophoretically aligned cell membranes prior to application of the high field pulse. The fusion observed due to AC fields in excess of 0.7 kV/cm presumably results from excessive dielectrophoretic force. An intercellular separation of 5 nm or less can be maintained for up to 10 sec following pulse application, possibly through the adhesive nature of the observed point defects and discontinuous area interactions. Cells not treated with pronase have less opportunity to develop temporary contacts which may subsequently develop into fusion sites. Pronase treatment has been shown to greatly enhance electrofusion yields (Zimmermann & Vienken, 1982), an effect mainly attributed to proteolytic action and Ca^{2+} contaminants (Ohno-Shosaku & Okada, 1984). The effects of pronase on human erythrocytes are well documented (Bender et al., 1971; Cabantchik & Rothstein, 1974).

Because the discontinuous areas emerge independently of pronase treatment and dielectrophoresis, and are not observed using much lower voltages (*unpublished results from this lab*), they must be considered a direct result of the high field pulse. The highly unstable nature of these defects is evidenced by their rapid reannealing in the 0.1 to 10 sec following the high field pulse application. Point defects, or lipidic particles, have been suggested to represent intermembrane contact sites in phospholipid model systems by various authors (Hui et al., 1981; Verkleij, 1984). In the case of electrofusion, their lifetime (0.1 to 10 sec) is short as compared to those observed in certain lipid mixtures.

The fusion observed does not appear to depend on a type of large scale segregation of intramembranous proteins commonly associated with polyethylene-glycol-induced fusion (Hui et al., 1985). The fact that many of the discontinuous areas are IMP-free suggests that the distortion and/or breakdown of membrane may occur more readily near the

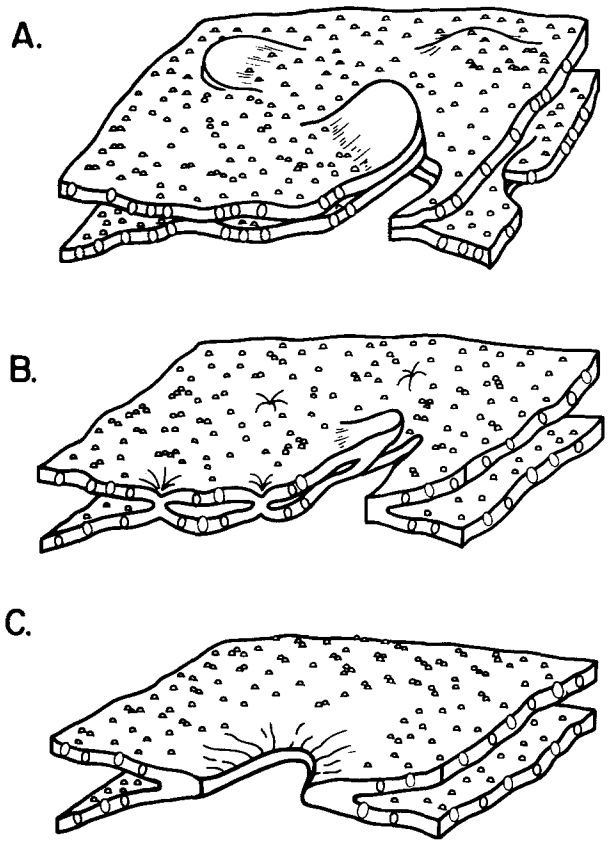

Fig. 9. Proposed ultrastructural model of electrofusion of membranes following pulse application. (*A*) Within 100 msec, adjacent cells reversibly rupture near the boundaries of IMP-sparse regions, separately, or in contact with a similar defect on an adjacent membrane. (*B*) At 2 sec, membrane continuity develops between contacting discontinuous areas. (*C*) From 10 sec on, cytoplasmic bridges expand to form permanent lumens

boundaries of small, randomly occurring IMP-free patches, as previously suggested (Pilwat et al., 1975), and perhaps to some extent that IMPs are excluded from the discontinuous areas as they develop. Based on a diffusion coefficient for erythrocyte membrane protein of about 10^{-11} cm^2/sec (Peters et al., 1974; Fowler & Branton, 1977), it would take seconds for IMPs to diffuse away from or return to discontinuous areas 50 to 150 nm in diameter. Since discontinuous areas were developed within 100 msec after the pulse, the exclusion of IMPs from the areas as they develop seems less likely.

We construct a model of events of human erythrocyte electrofusion by a single pulse as shown in Fig. 9. Within 100 msec of the pulse, small, mostly IMP-free patches are forced from the plane of the membrane. Most of the resulting discontinuous areas of 50 to 150 nm across reanneal within 2 sec, unless they contact another defect on an adjacent membrane, whereby fusion is initiated (Fig. 9*A*). Other areas of the membrane which are forced into contact may form transient attachment sites (Fig. 9*B*). IMPs then may diffuse through all areas except along the fusion sites where two membranes are irreversibly attached. After 10 sec, most of the transient attachment sites vanish, but a few fused gaps continue to develop into cytoplasmic bridges, the edges of which show continuous P- and E-membrane fracture faces of fused, adjacent cells (Fig. 9*C*).

Our results support the model of Zimmermann (1982) in that regions of the membrane free of integral proteins appear to be the sites where fusion was initiated. The time span observed for the appearance of discontinuous areas qualitatively corresponds with the electropermeation results of Kinosita and Tsong (1979). Because the long-lived "pores" of diameter <2 nm would not be observable by freeze-fracture electron microscopy, our observation of morphological perturbation may indicate a different type, or stage, of membrane defect than those responsible for solute permeation over the course of several hours.

We wish to thank Dr. A. Sen for helpful discussions, and Mr. W. Beers for switching circuit design and technical assistance. This study was supported by NIH grant GM30969.

References

Bender, W.W., Garan, H., Berg, H.C. 1971. Proteins of the human erythrocyte membrane as modified by pronase. *J. Mol. Biol.* **58**:783–797

Benz, R., Beckers, F., Zimmermann, U. 1979. Reversible electrical breakdown of lipid bilayer membranes: A charge-pulse relaxation study. *J. Membrane Biol.* **48**:181–204

Blangero, C., Teissie, J. 1983. Homokaryon production by electrofusion: A convenient way to produce a large number of viable mammalian cells. *Biochem. Biophys. Res. Commun.* **114**:663–669

Buschl, R., Ringsdorf, H., Zimmermann, U. 1982. Electric field-induced fusion of large liposomes from natural and polymerizable lipids. *FEBS Lett.* **150**:38–42

Cabantchik, Z.I., Rothstein, A. 1974. Membrane proteins related to anion permeability of human red blood cells. II. Effects of proteolytic enzymes on disulfonic stilbene sites of surface proteins. *J. Membrane Biol.* **15**:227–248

Costello, M.J., Corless, J.M. 1978. The direct measurement of temperature changes within freeze-fracture specimens during rapid quenching in liquid coolants. *J. Microsc. (Oxford)* **112**:17–37

Dimitrov, D.S., Jain, R.K. 1984. Membrane stability. *Biochim. Biophys. Acta* **779**:437–468

Fairbanks, G., Steck, T.L., Wallach, D.F. 1971. Electrophoretic analysis of the major polypeptides of the human erythrocyte membrane. *Biochemistry* **10**:2606–2616

Fowler, V., Branton, D. 1977. Lateral mobility of human erythrocyte integral membrane proteins. *Nature (London)* **268**:23–26

Hui, S.W., Isac, T., Boni, L.T., Sen, A. 1985. Action of polyethylene glycol on the fusion of human erythrocyte membranes. *J. Membrane Biol.* **84:**137–146

Hui, S.W., Stewart, T.P., Boni, L.T., Yeagle, P.L. 1981. Membrane fusion through point defects in bilayers. *Science* **212:**921–923

Kinosita, K., Tsong, T.Y. 1979. Voltage-induced conductance in human erythrocyte membranes. *Biochim. Biophys. Acta* **554:**479–497

Lo, M., Tsong, T.Y., Conrad, M.K., Strittmatter, S.M., Hester, L.D., Snyder, S.H. 1984. Monoclonal antibody production by receptor-mediated electrically induced cell fusion. *Nature (London)* **310:**792–794

Ohno-Shosaku, T., Okada, Y. 1984. Facilitation of electrofusion of mouse lymphoma cells by the proteolytic action of proteases. *Biochem. Biophys. Res. Commun.* **120:**138–143

Peters, R., Peters, J., Tews, K.H., Bahr, W. 1974. A microfluorometric study of translational diffusion in erythrocyte membranes. *Biochim. Biophys. Acta* **367:**282–294

Pilwat, G., Zimmermann, U., Riemann, F. 1975. Dielectric breakdown measurements of human and bovine erythrocyte membranes using benzyl alcohol as a probe molecule. *Biochim. Biophys. Acta* **406:**424–432

Rand, R.P. 1981. Interacting phospholipid bilayers. Measured forces and induced structural changes. *Annu. Rev. Biophys. Bioeng.* **10:**277–314

Schwister, K., Deuticke, B. 1985. Formation and properties of aqueous leaks induced in human erythrocytes by electrical breakdown. *Biochim. Biophys. Acta* **816:**332–348

Sowers, A.E. 1983. Fusion of mitochondrial inner membranes by electric fields produces inside-out vesicles. Visualization by freeze-fracture electron microscopy. *Biochim. Biophys. Acta* **735:**426–428

Sowers, A.E. 1984. Characterization of electric field-induced fusion in erythrocyte ghost membranes. *J. Cell Biol.* **99:**1989–1996

Sowers, A.E. 1985. Electric field induced fusion in erythrocyte ghosts: Evidence that pulses induce a long-lived fusogenic state and that fusion may not involve pore formation. *Biophys. J.* **47:**171a (*Abstr.*)

Teissie, J., Tsong, T.Y. 1980. Evidence of voltage-induced channel opening in Na/K ATPase of human erythrocyte membrane. *J. Membrane Biol.* **55:**133–140

Verkleij, A. 1984. Lipidic intramembranous particles. *Biochim. Biophys. Acta* **779:**43–63

Vienken, J., Zimmermann, U., Ganser, R., Hampp, R. 1983. Vesicle formation during electrofusion of mesophyll protoplasts of *Kalanchoe diagremontiana*. *Planta* **157:**331–335

Weaver, J.C., Powell, K.T., Mintzer, R.A., Ling, H., Sloan, S.R. 1984. The electrical capacitance of bilayer membranes. The contribution of aqueous pores. *Bioelectrochem. Bioelectroenerg.* **12:**394–404

Zimmermann, U. 1982. Electric field-mediated fusion and related electrical phenomena. *Biochim. Biophys. Acta* **694:**227–277

Zimmermann, U., Vienken, J. 1982. Electric field-induced cell-to-cell fusion. *J. Membrane Biol.* **67:**165–182

Received 18 February 1986; revised 28 April 1986